1985RMxAA..10..229S

THE IUE SPECTRUM OF AX MONOCEROTIS

Jorge Sahade[1,3] and Estela Brandi[2,4]

RESUMEN. Imágenes de AX Monocerotis obtenidas en alta dispersión con el satélite ultravioleta IUE, en una sola fase del ciclo orbital, han sido analizadas desde el punto de vista del espectro continuo así como del espectro de líneas. El continuo corresponde al de la componente temprana del sistema. Se da una lista de identificaciones del espectro de líneas y se propone un modelo para la envoltura extendida.

ABSTRACT. High dispersion IUE images of AX Monocerotis, secured at one single phase of the orbital cycle, were analyzed for the continuous as well as for the line spectrum. The continuum corresponds to that of the early type component of the system. A list of line identification is given and a model is proposed for the extended envelope.

I. INTRODUCTION

AX Monocerotis [HD 45910 = BD + 5°1267 = SAO 113974; $\alpha = 6^h\ 27^m\ 52^s$, $\delta = +5°54'.1$ (1950.0); V = 6.59-6.88 mag.] is a binary system with a B3nn and a K0 III components, the orbital period being 232.5 days, and the rotational velocity of the early-type star, 345 km/s (Cowley 1964). According to Cowley's orbital elements, periastron passage occurs a few hundredths of the period after the quadrature at which the late-type component, in its orbital motion, reaches the maximum velocity of recession.

The photographic spectrum can be described as displaying (cf. Cowley 1964)

a) lines of the two stellar components;

b) P Cygni profiles in H (and occasionally in He I), the absorption being variable & from time to time becoming double or multiple, the velocities being of the order of -150 and -250 km/s, respectively.

c) *on rare occasions*, weak absorptions of Ni II 4067 and Fe II 4233 with the same displacements as the H lines;

d) weak, hazy emission of Fe II;

e) occasional, faint |Fe II| (essentially 4244) emission, varying from hazy to reasonably sharp, the average velocity being +1.4 km/s;

f) structure in the resonance lines of Ca II and Na I: an interstellar feature, one or more components with the same displacements as the H P Cygni absorptions, and a shell component [cf. g)];

g) a shell-like spectrum displaying Mg I, Mg II, Si I, Si II, Sc II, Ti II, Cr II, Fe I, Fe II and Ni II, which is present from some 7 weeks before to a few weeks after the conjunction at which the B star is behind; the velocities are of recession, before conjunction, and of approach, after conjunction.

[1] Instituto Argentino de Radioastronomía, Argentina

[2] Observatorio Astronómico, La Plata, Argentina

[3] Member of the Carrera del Investigador Científico, CONICET, Argentina. Guest Observer, International Ultraviolet Explorer

[4] Member of the Carrera del Investigador Científico, CIC, Argentina

The shell lines have been interpreted as being produced by an eclipse of the B star by an extended atmosphere around the K component, and by the presence of a gaseous stream from the latter object towards the early-type companion.

When the shell spectrum is present, the hazy Fe II emission appears as double because of the absorption effect of the corresponding Fe II shell line, thus suggesting that the Fe II emission arises in a region around the B star or between the two components of the system.

Struve (1943), the Burbidges (1954) and Cowley (1964) have called attention to the fact that sometimes the violet Hε absorption is suppressed, with no reasonable explanation so far offered.

Cowley's derived orbital elements are

K_K = 51.5 km/s

γ = + 6.5 km/s

e = 0.02

$a \sin i$ = 1.64×10^8 km

$f(\mathcal{M})$ = $3\ \mathcal{M}_\odot$.

From the velocities derived from the lines of the early-type component it would appear that the masses should be $8.6\mathcal{M}_\odot$ for the B component and $3.4\mathcal{M}_\odot$ for the K companion, if an inclination of 65° is adopted. If these were the values of the masses, the separation of the components would be of the order of 300 $R_\odot$.

AX Mon has been found to have intrinsic polarization (cf. Serkowski 1970, Pfeiffer and Koch 1977). The object was not detected as a radio source at 10.6 GHz (Woodsworth and Hughes 1977) and is not known to be an X-ray source either.

AX Mon was considered by Swings (1970) as a symbiotic-related star. In fact, we are dealing here with a *combination spectrum* -an early-type object, although not a sudwarf, and a late-type giant, although earlier than M- and an orbital period similar to those one finds among symbiotic binaries. The study of AX Mon, therefore, could throw light on the evolutionary history of symbiotic stars. As a consequence, one of us (J.S.) included this binary in his observing program of symbiotic stars with the IUE satellite, in January, 1979. The high dispersion images that were obtained are listed in Table 1; they were secured with large aperture from the NASA IUE ground observatory at the Goddard Space Flight Center, in Greenbelt, Maryland, U.S.A. Unfortunately, there are no observations in other wavelength ranges simultaneous or contemporaneous with our IUE observations.

TABLE 1

IUE IMAGES OF AX MONOCEROTIS

Image*	U.T. of Start of Exposure Year	Day	Hour	Minutes	Exposure Time (Minutes)	Phase** (P)
SWP 3374	1979	1	21	12	65	0.095
LWR 3353	1979	1	22	24	20	0.095

* SWP: short wavelength prime camera; range: 1165-2126 Å
LWR: long wavelength redundant camera; range: 1845-3230 Å
** The phases were computed from the expression
2,433,390.8 + 232.5 days
given by Cowley (1964) for the time of periastron passage.
If we take as origin the conjunction at which the K component is in front, the phase of the two images is 0.38 P.

II. THE CONTINUUM SPECTRUM

In a previous paper (Sahade, Brandi and Fontenla 1984) on the IUE observations of symbiotic objects, we have reported on the fitting with Kurucz's (1979) LTE model atmosphere calculations of the ultraviolet continuum of AX Mon, calibrated, in absolute flux units, with the use of the method suggested by Cassatella *et al.* (1981). The fitting was good for T_e=20000° K and $\log g \sim 2.5$. The temperature is what we would have for spectral type around B2, and the gravity value would suggest that we are dealing with a giant object. Therefore, the fitting with Kurucz's models would describe the ultraviolet continuum of AX Mon as that of a B2 (or B3) III object, in coincidence with the listing of the star by Batten, Fletcher and Mann (1978), but at variance with the suggestion from the photographic spectrum that we are dealing with a main sequence star (Struve 1943).

III. THE LINE SPECTRUM

The ultraviolet line spectrum of AX Mon is essentially one of absorption features, except in the case of the resonance lines of Mg II at 2800 Å which display a P Cygni profile. Table 2 lists the identifications made.

TABLE 2

ULTRAVIOLET LINES IN THE SPECTRUM OF AX MON

		IDENTIFICATIONS			
λ obs. (Å)	FWHM (Å)	ELEMENT	MULT.	λ lab. (Å)	INT:
1188.9		SiII	5	1190.42	100
1189.4		SIII	1	1190.17	200
1189.8					
1190.45	0.1	SIII	1	1190.17	200
1190.55	0.1	SiII	5	1190.42	100
1192.5		SiII	5	1193.289	200
		SIII	1	1194.02	400
1193.5		SiII	5	1194.500	250
		SIII	1	1194.02	400
				94.40	300
1196.0	1.5	SiII	5	1197.394	100
1196.6					
1197.0					
1200.0	4.0	SIII	1	1200.97	400
				01.71	200
				02.10	50
		NI	1	1199.549	1000
				1200.224	950
				.711	700
1226.4		SiII	8.02	1227.604	100
1228.0		SiII	8.01	1228.746	150
1228.8		SiII	8.01	1229.388	200
1229.9		NiII		1231.041	100
1230.3					
1232.5		?			
1235.5		?			
1238.8	2.5	NV	1	1238.821	1000
1242.8	1.3	NV	1	1242.804	800
1247.5		SiII	8	1246.738	100
1249.2	1.5	SiII	13.05	1250.09	150
1249.6				1250.09	100
1250.0		SII	1	1250.50	300
1250.7	0.2	SII	1	1250.50	300
1252.4	1.5	SII	1	1253.79	500
1252.9					
1253.3					
1253.9	0.2	SII	1	1253.79	500
1259.0	2.4	SiII	4	1260.42	500
		SII	1	1259.53	500
		FeII	9	1260.542	400
1260.55	0.4	SiII	4	1260.42	500
		FeII	9	1260.542	400
1263.3	2.0	SiII	4	1264.74	1000
1263.7				1265.00	100
1264.35					
1266.6		FeII	9	1267.43	500
1266.95					
1267.7		?			
1268.4					
1268.7					
1271.5	1.5	FeII	9	1272.0	500
				1272.64	300
1275.0		FeII	9	1275.80	400
1275.4					
1277.2		CI	7	1277.282	700
				1277.245	300
1277.35		CI	7	1277.55	1000
1277.6		CI	7	1277.72	250
1280.0		CI	5	1279.89	250
1280.25	0.1	CI	5	1280.33	700
1281.9		TiIII	2	1282.48	125
1283.65		NiII:		1284.327	25
1285.8	0.9	TiIII	2	1286.365	700
1288.65	0.6	TiIII	2	1289.30	500
1290.9	0.9	TiIII	2	1291.62	450
		FeII	9	1291.714	600
		FeII	9	1291.618	300
1292.7	0.5	TiIII	2	1293.23	400
		FeII	9	1293.661	200
1293.9	1.4	TiIII	1	1294.70	600
1295.8	1.3	TiIII	1	1295.88	400
		FeII	86	1296.088	400
1298.0		TiIII	1	1298.66	1000
		TiIII	1	1298.97	800
1298.8	1	TiIII	1	1298.66	1000
1301.2	2.2	OI	2	1302.17	1000
1302.3		OI	2	1302.17	1000
1303.08		OI	2	1304.86	600
		SiII	3	1304.37	100
1304.45:		SiII	3	1304.37	100
1305.15		OI	2	1306.03	200
1307.85	1.6	SiII	3	1309.28	200
1308.2					
1308.6					
1310.0		PII	2	1310.70	600
1312.5		?			
1315.75	1.2	NiII	10	1317.220	500
1316.4					
1316.8					
1317.35	0.1	NiII	10	1317.220	500
1318.45		NI	12	1318.998	150
1318.85		NI	12	1319.005	80
1319.25		NI	12	1319.676	250
1323.7		CII	11	1323.95	450
		CII	11	1323.9	300
1327.0		TiIII	4	1327.59	550
1328.95	0.15	CI	4	1329.10	200
		CI	4	1329.09	150
1329.2	0.15	CI	4	1329.58	600
1334.0	3.0	CII	1	1335.71	1000
		CII	1	1334.53	800
		CII	1	1335.66	100
		PIII	1	1334.87	650

TABLE 2 (continued)

λ obs. (A)	FWHM (A)	IDENTIFICATIONS			
		ELEMENT	MULT.	λ lab. (A)	INT.
1335.8	0.2	CII	1	1335.71	1000
1343.7		PIII	1	1344.34	1000
		PIII	1	1344.90	650
1346.4		SiII	7	1346.873	100
1347.35		SiII	7	1348.54	100
1347.85					
1348.15					
1349.5		SiII	7	1350.057	150
1352.2		SiII	7	1352.635	100
1353.15		SiII	7	1353.718	100
1358.45		?			
1360.45		FeII		1361.372	85
1360.95		SiIII	46	1361.597	160
		NiII		1361.885	50
1362.5		SiIII	38	1363.459	140
1363.6		FeII	103	1364.575	240
1364.0					
1366.0		SiIII	46	1367.049	140
1367.5		FeII		1368.098	50
1368.8	0.8	NiII	8	1370.136	500
1369.3					
1369.5					
1370.2	0.15	NiII	8	1370.136	500
1371.85		FeII	85.07	1372.292	6 J
1373.3		NiII	9	1374.075	150
1374.2		FeII		1375.172	200
1374.7					
1378.9		PIII	7	1379.87	500
1380.15		PIII	7	1380.46	1000
1380.55		PIII	7	1381.11	1000
1380.85		PIII	7	1381.63	800
		NiII	8	1381.295	200
1393.6	4.1	SiIV	1	1393.76	1000
1398.3		NiII	8	1399.026	80
1402.6	3.7	SiIV	1	1402.77	800
1405.1		?			
1407.9		FeII.		1408.478	80
1409.8		NiII		1411.071	100
1410.25					
1410.6					
1412.1		FeII	60	1413.699	70
1412.4		FeII	46.07	1412.867	8 J
		FeII	47	1412.842	8 J
1413.7		?			
1415.0		NiII		1416.06	12
		NiII		1415.73	20
1416.9	1.7	FeII	143	1417.744	400
1419.8		TiIII		1420.036	300
		TiIII		1420.440	280
1420.7		TiIII		1421.631	280
1421.2		TiIII		1421.767	250
1421.7		TiIII		1422.405	650
1423.7		FeII	47	1424.716	70
		FeII	47	1424.047	50
		TiIII		1424.140	300
1429.85		FeII		1430.780	200
1430.5		FeII		1430.895	120
1434.3		FeII	47	1434.996	70
1446.0	4.0	?			
1453.3		TiIII	5	1455.19	1000
1454.0		NiII	7	1454.852	200
1454.4					
1455.9		NiII		1456.913	16
1464.15		FeII	193	1465.043	400
1464.5					
1466.4		NiII	6	1467.762	100
1466.6					
1466.85					
1468.0		NiII	6	1467.762	100
1485.6		FeIII	85	1486.265	450
1491.85		NI	4	1492.64	620
1492.05		NI	4	1492.82	100
		FeIII	85	1493.640	600
1493.9		NI	4	1494.68	400
		FeII	316.04	1494.776	3 J
1494.3		FeIII		1495.210	70
		NiII		1495.383	40
1498.0		TiIII	3	1498.70	600
1498.75		TiIII		1499.173	300
1499.6		NiII	7	1500.651	200
1501.4		PIII	6	1501.55	700
		PIII	6	1302.27	1000
		TiIII		1502.311	200
1503.5		PIII	6	1504.72	900
		TiIII		1504.621	120
1504.4		FeIII	85	1505.166	650
1509.6		NiII	6	1510.859	75
1510.0					
1510.4					
1525.15	1.5	SiII	2	1526.71	500
1525.6					
1526.05					
1526.8	0.3	SiII	2	1526.71	500
1532.3	1.7	SiII	2	1533.43	1000
1537.5		FeIII	84	1538.632	650
1538.1		FeIII	84	1539.128	550
			84	1539.480	300
1549.7	6.1	CIV	1	1548.19	1000
		CIV	1	1550.77	950
1558.1		FeII	45	1559.084	400
1558.55		FeII	46	1558.542	200
		FeII	46	1558.690	200
1560.5		CI	3	1560.68	500
		CI	3	1560.71	200
1560.9		CI	3	1561.44	1000
1561.5		FeII	68.01	1562.270	4 J
1561.9					
1562.8		FeII	45	1563.79	500
1563.2					
1565.8		FeII	44	1566.82	400
1566.35					
1568.6		FeII	44	1569.67	240
1569.2		FeII	45	1570.25	400
1569.7					
1573.4		FeII	44	1574.77	400
1573.8		FeII	45	1574.93	400
1576.4		FeII	45	1577.166	20
1576.7					
1577.6		FeII.	68.01	1578.219	2 J
1577.8					
1579.6		FeII	44	1580.625	500
1580.0					
1584.0		FeII	44	1584.95	300
1584.4					
1585.5		FeII		1585.985	30
1587.2		FeII	44	1588.286	200
1587.5					
1597.7		ScIII:	1	1598.002	160
1601.4		FeIII	119	1602.00	300
1602.0		ScIII	1	1603.064	360
1604.8		NiII		1605.910	60
1605.3		FeIII		1606.014	200
1606.6		FeIII	118	1607.723	600
1607.35	1.1	FeII	8	1608.456	700
1607.85					
1608.6	0.2	FeII		1608.456	700
1610.0		FeII	43	1610.923	300
				1610.933	300
1611.9		FeII	43	1612.81	400
1612.2					
1613.5		NiII		1614.911	90
1614.0		NiII		1615.459	120
1614.4					
1615.8		NiII		1617.088	50
1616.2		NiII		1617.144	40
1616.8		NiII		1617.299	40
1617.5		FeII	8	1618.47	500
1617.9					
1620.7	1.0	FeII	8	1621.685	600
1621.1					
1622.15		FeII	43	1623.091	160
1622.5					
1623.7		FeIII		1624.206	150

TABLE 2 (continued)

		IDENTIFICATIONS			
λ obs. (A)	FWHM (A)	ELEMENT	MULT.	λ lab. (A)	INT.
1624.5		FeII	43	1625.520	400
1624.9		FeII	8	1625.909	300
1625.3		AlII	9	1625.627	150
1628.1	1.0	FeII	8	1629.154	600
1628.5					
1630.1		FeII	8	1631.12	600
1630.45					
1631.5		FeII	43	1632.667	20
1631.8		NiIII	17	1632.166	100
1632.0		NiII		1632.171	30
1632.8		FeII	43	1633.908	300
1633.4		FeII	8	1634.345	400
1633.7					
1634.4		FeII	68	1635.398	700
1634.8					
1635.15		FeII	8	1636.321	600
1635.7					
1636.4		FeII	42	1637.397	300
1636.9		NiII		1637.589	300
		NiII		1637.439	100
1638.35		FeII	8	1639.403	600
1638.85					
1639.5		FeII	43	1640.150	240
1640.6		FeII	68	1641.76	500
1641.1					
1642.6		FeII	42	1643.576	300
1643.0					
1645.2		FeII	68	1646.182	400
1645.6					
1646.1		FeII	68	1647.159	500
1646.6					
1648.5		FeII	68	1649.572	400
1649.0		FeII	42	1649.426	300
1653.5		FeII	68	1654.105	100
1653.9		FeII	42	1654.476	100
1656.4		CI	2	1656.27	350
		CI	2	1656.93	300
1657.1	0.4	CI	2	1657.01	1000
1657.6		CI	2	1657.38	300
1658.2		FeII	40	1659.487	400
1658.9					
1660.6		FeII	41	1661.347	5 J
1662.1		FeII	40	1663.221	300
1662.6					
1669.5	1.6	AlII	2	1670.787	1000
		FeII	40	1670.742	500
1670.9	0.3	AlII	2	1670.787	1000
1672.4		FeII	102	1673.462	300
1672.9					
1673.8		FeII	40	1674.716	80
1674.1		FeII	41	1674.440	40
1676.0		FeII	41	1676.853	20
1678.3		FeII	102	1679.381	300
1678.7					
1680.5:		FeII	40.01	1681.111	1 J
1685.4		FeII	40	1686.455	160
1685.9					
1687.3		NiIII	25	1687.897	400
1691.9		NiIII	16	1692.514	1000
1694.2	1.3	FeIII		1695.036	150
1695.65		FeII	38	1696.794	160
1696.15					
1698.0		FeII	85	1699.193	40
1700.9		FeII	38	1602.045	500
1701.45					
1702.3		NiII	5	1703.408	25
1702.6		NiIII	16	1703.467	50
1702.9					
1703:6		NiII	5	1703.408	25
1706.8					
1707.6					
1708.0		NiII	4	1709.598	200
1708.6		FeII	84	1709.670	300
1709.05		NiIII	16	1709.901	800
1709.8		NiII	4	1709.598	200
1714.5		FeII	84	1715.503	240
		NiIII	16	1715.303	650
1715.4		FeII	39	1716.577	40
1716.0					
1717.2		FeII	38	1718.123	40
1717.5					
1718.6		NiIII	16	1719.458	500
1719.4		FeII	38	1720.621	400
1719.6		FeII	84	1720.042	200
1720.1		AlII	6	1721.27	900
1720.4		AlII	6	1721.24	500
		CII:	14.02	1721.68	200
				1721.01	100
1722.0		FeIII		1722.837	250
1724.1	1.2	AlII	6	1724.98	900
				1724.95	500
		FeII	37	1724.966	160
		FeII	39	1724.854	160
1725.3		FeII	38	1726.391	240
1725.75					
1730.0		FeII	110	1731.038	200
1730.4					
1737.1		NiIII	15	1738.252	500
1737.8		NiIII	28	1738.785	300
1740.1	1.1	NiII	5	1741.547	1000
1740.5					
1740.8					
1741.7		NiII	5	1741.547	1000
1746.2		NiIII	15	1747.011	550
1746.7		NiII	5	1748.285	500
1747.2					
1747.7					
1750.4	1.1	NiII	4	1751.911	300
1750.7					
1751.2					
1752.0		NiII	4	1751.911	300
1753.7		NiII	4	1754.808	50
1759.3		AlII	5	1760.10	350
		FeII	100	1760.415	400
1760.2		FeII	101	1761.379	500
1761.0		AlII	5	1761.98	300
1763.1		AlII	5	1763.95	700
				1763.87	500
1764.0		NiIII	14	1764.688	800
1765.0		AlII	5	1765.82	300
1766.9		AlII	5	1767.73	400
		NiIII	14	1767.938	500
1769.0		NiIII	14	1769.643	1000
1769.3		FeIII		1770.247	200
1769.8		FeIII		1770.554	400
1770.35		NiIII	14	1771.492	100
1771.3		FeIII		1771.975	150
1771.5		FeII	99	1772.509	300
1771.85					
1772.8		NiII	3	1773.949	25
		NiIII	27	1773.788	40
1775.1		FeIII		1775.983	400
		NiIII		1776.068	400
1780.6		FeII	67	1781.702	40
1782.2		NiIII	14	1782.747	60
1784.05	1.0	FeII	191	1785.26	800
1784.6					
1785.75	1.0	FeII	191	1786.74	800
1786.15					
1787.0	1.0	FeII	191	1788.07	700
1787.4		NiII	5	1788.485	100
1790.5		NiIII	14	1791.644	200
1792.3		FeII	99	1793.367	200
1792.7					
1794.2		NiIII	14	1794.904	200
1797.3		FeII	142	1798.150	200
1806.0	1.3	SiII	1	1808.01	150
1806.8					
1807.2					
1808.2	0.25	SiII	1	1808.01	150
1810.9		FeIII		1811.924	200
1811.2				1811.689	200
1811.4		NiII	24	1812.065	30

TABLE 2 (continued)

		IDENTIFICATIONS			
λ obs. (A)	FWHM (A)	ELEMENT	MULT.	λ lab. (A)	INT.
1814.85 1815.6 1816.1	1.9	SiII	1	1816.93	200
1821.2 1821.5		FeII	66	1822.150	20
1822.0		NiIII	20	1823.061	800
1829.7		FeIII	117	1830.623	200
		NiIII	20	1830.006	400
				1830.075	200
1831.0		?			
1832.9		FeIII		1834.096	70
1834.5 1834.9		FeII	98	1835.874	300
1837.5		FeIII	117	1838.309	450
1840.5 1840.9		FeII	65	1841.701	200
1842.9:		FeIII	117	1843.502	150
1844.3		FeIII	117	1845.304	300
			97	1845.521	450
1845.9		FeII	98	1846.573	240
1846.5		NiIII	19	1847.275	650
1853.6		AlIII	1	1854.716	1000
		FeIII	63	1854.826	600
				1854.975	300
		NiIII	19	1854.149	800
1855.9		FeIII	63	1856.690	450
1857.4		FeIII	63	1858.542	300
1859.1		FeIII	63	1859.955	200
		FeII	65	1859.741	300
		FeII	97	1860.055	400
1861.5		AlIII	1	1862.790	600
		AlII	4	1862.311	1000
1862.6		AlIII	1	1862.790	600
1864.1		FeII	126	1864.743	400
1865.5		FeIII	52	1866.305	600
				1866.554	300
1869		FeIII	52	1869.828	650
1870.3		FeIII	52	1871.152	600
1871.7		FeIII		1872.214	400
		FeIII		1872.52	250
1881.35		FeIII	62	1882.047	650
1883.8		FeIII	96	1885.125	600
		FeIII	62	1884.596	550
1885.8		FeIII	52	1886.757	800
1886.4		FeIII	52	1887.471	550
		FeIII	53	1887.197	550
1889.6		FeIII	52	1890.669	900
1891.1		FeIII	96	1892.247	300
				1892.073	300
		FeIII	52	1892.140	300
1894.0		FeIII	34	1895.46	1000
		FeII	124	1895.675	200
1896.0		FeIII	83	1896.803	600
1898.1		FeIII	96	1899.318	300
1906.9		FeIII	83	1907.577	650
				1907.741	250
1909.7		FeIII	57	1910.401	400
1912.7		FeIII	57	1913.622	250
		FeIII	34	1914.056	1000
1916.7		FeIII	101	1917.453	600
			95	1917.351	550
			108	1917.087	150
		FeII	96	1917.337	300
1917.4		FeIII	108	1918.480	450
			57	1918.284	450
1919.0		FeIII	95	1920.186	250
1921.9		FeIII	51	1922.79	1000
			95	1923.003	450
		FeII	138	1922.797	400
1924.7		FeII	123	1925.983	400
1936.3	1.8	FeIII	51	1937.34	950
		FeII	96	1936.799	400
1938.2		FeIII	106	1938.901	650
1939.25		FeIII	61	1940.018	550
1940.7		FeIII	79	1941.633	200
1942.5		FeIII	51	1943.48	950
1944.4		FeIII	61	1945.342	800
1950.0		FeIII	68	1951.007	800
				1951.318	200
1952.0:		FeIII	68	1953.322	900
1962.3		FeII	170	1963.110	500
1963.5		FeIII	82	1964.169	550
				1964.776	550
				1964.019	300
			61	1964.260	450
		FeII	170	1964.342	240
1964.2		FeIII	106	1965.309	550
1975.3	1.4	FeIII	54	1976.126	550
1977.6		FeIII	54	1978.417	250
1979.3		FeIII		1980.392	150
1981.4		FeIII	54	1982.076	400
1992.3		FeIII	50	1993.262	450
		ScIII:	4	1993.886	180
1993.2		FeIII	50	1994.073	900
1994.0		FeII	228	1994.857	400
		FeIII	50	1995.266	450
				1995.563	800
1995.5		FeIII	50	1996.420	800
1998.8		FeII	187	1999.430	200
1999.6		FeII	186	1999.462	150
2000.3		FeIII:	55	2001.167	25
2003.4		NiII	33	2004.266	50
2005.0		FeIII	55	2006.265	25
2006.3		FeIII	55	2007.845	90
		FeII	83	2007.452	150
				2007.013	120
2007.6		FeIII	55	2008.469	40
		FeII	83	2008.358	
				2008.090	
2024.8	1.5	ZnII	1	2025.486	300
		MgI	2	2025.824	35
2026.3 2026.6		FeII	186	2027.778	50
2028.6 2029.1		FeII	93	2029.182	80
2031.9 2032.3		FeII	94	2032.407	250
2036.2		?			
2055.7		FeIII	71	2056.145	120
2061.0		ZnII	1	2062.003	300
		CrII	1	2061.54	175
		FeIII	48	2061.552	250
2062.4		ZnII	1	2062.003	300
2062.85		FeII	92	2063.672	250
2067.25	2.7	FeIII	48	2068.243	350
2089.5	1.7	FeIII	67	2090.139	350
2090.8		FeIII	77	2091.312	120
2092.9		FeII	290	2093.711	50
2093.25					
2097.0	2.1	FeIII	67	2098.149	570
			66	2098.361	350
		FeII	120	2098.176	250
2160.3		NiII	14	2061.217	80
2164.3		NiII	13	2165.55	320
2168.0		NiII	13	2169.096	440
2173.5		FeIII	70	2174.658	570
		NiII	14	2174.666	440
2176.25		NiII	40	2177.086	220
				2177.361	200
2179.3		NiII	40	2180.473	280
		FeIII	70	2180.410	350
2183.5		NiII	13	2184.60	280
2200.2		NiII	13	2201.409	240
2205.5		NiII	13	2206.715	620
2209.0		NiII	13	2210.382	180
2215.0		NiII	12	2216.482	800
2219.3		NiII	28	2220.402	280
2221.6		NiII	12	2222.957	300
2243.2		?			
2252.5		NiII	12	2253.848	220
2263.5		NiII	12	2264.461	320
2268.7 2269.5		NiII	12	2270.214	440
2275.0		NiII	39	2275.684	180

TABLE 2 (continued)

		IDENTIFICATIONS			
λ obs. (A)	FWHM (A)	ELEMENT	MULT.	λ lab. (A)	INT.
2277.6		NiII	22	2278.770	280
2286.0		NiII	38	2287.648	220
			22	2287.089	180
2295.5		NiII	21	2296.552	200
2297.5		NiII	21	2298.270	180
2298.9		NiII	27	2299.651	140
2301.9		NiII	11	2302.996	320
			59	2302.479	140
2307.7		NiII	50	2308.518	120
2311.4		NiII	58	2312.916	140
2314.4		NiII	11	2316.039	320
2318.0		NiII	37	2319.750	220
2326.0		FeIII	121	2326.948	250
2331.4		FeII	3	2332.80	170
2333.1		NiII	20	2334.524	220
2336.7 2337.8		FeII	3	2338.007	140
2340.0		NiII	50	2341.202	220
2342.0		FeII	3	2343.494	240
2343.4 2343.8		FeII	3	2344.281	125
2347.0		FeII	36	2348.113	140
			3	2348.299	155
2350.5		FeII:	379	2351.666	15
2353.6		FeII:	165	2354.477	50
2358.4		FeII	3	2359.118	140
			165	2359.111	285
			379	2359.118	140
2359.0 2359.4		FeII	35	2359.997	125
			36	2360.293	110
2363.4 2364.0		FeII	3	2364.826	140
2372.2 2373.0		FeII	2	2373.735	125
2374.0		NiII	21	2375.418	320
2378.4 2379.3		FeII	3	2380.762	110
2380.5 2381.3		FeII	2	2382.03	320
2382.3		?			
2387.0 2387.7		FeII	2	2388.63	170
2393.6 2394.7	2.7	FeII	2	2395.63	320
2397.7 2398.5	1.5	FeII	2	2399.241	170
2403.4		FeII	2	2404.88	280
2405.0 2405.9		FeII	2	2406.660	155
2409.4		FeII	2	2410.52	170
2411.95 2412.6		FeII	2	2413.310	125
2414.9		NiII	20	2416.134	440
2422.3		FeII	301	2423.210	40
2427.6		FeII	300	2428.364	110
2428.5 2429.3		FeII	180	2430.078	110
2431.0 2431.5 2432.1		FeII	180	2432.262	80
			164	2433.495	70
		NiII	19	2433.556	100
2433.3 2434.1		FeII	321	2434.729	50
			375	2434.822	50
			180	2434.951	50
2436.4		NiII	19	2437.892	220
		FeII	375	2437.632	200
2437.5 2438.6		FeII	209	2439.302	125
2443.8		FeII	375	2444.274	100
			148	2444.515	100
2449.4		FeII	375	2450.134	50
			300	2450.205	25
2453.2 2453.9		FeII	2453.935		250
2457.3 2458.1		FeII	209	2458.784	125
2460.3 2461.1		FeII	209	2461.860	100
2462.5		FeII	208	2463.292	50
2463.5		FeII	208	2464.009	40
2464.25		FeII:	148	2465.199	10
2465.2		FeII	208	2465.912	50
2466.0		FeII	179	2466.819	60
2471.6 2472.2		NiII	19	2473.148	100
2478.7 2479.4		FeII	179	2480.115	285
2480.9 2481.45		FeII	207	2482.657	100
2482.8 2483.4		NiII	61	2484.204	140
2485.05 2485.55		FeII	208	2486.343	220
2488.5 2489.2		FeII	331	2490.706	100
2490.05 2490.6		FeII	207	2491.396	100
2491.7 2492.4		FeII	161	2493.262	220
2497.25 2498.05		FeII	161	2498.897	450
2502.2 2503.0		FeII	161	2503.560	110
2505.0		NiII	48	2505.843	120
2509.4		NiII	18	2510.871	220
2510.1 2510.9		FeII	161	2511.761	110
2513.75		NiII	61	2514.627	140
2514.9		?			
2515.2		TiIII	7	2516.053	1000
2515.65		?			
2516.5		FeII	147	2517.131	50
			207	2517.211	20
2518.25		FeII	268	2519.046	60
2520.4 2521.1		FeII	268	2521.092	40
			330	2521.816	30
2523.6 2524.5		FeII	159	2525.388	140
		NiII	61	2525.296	180
2528.0 2528.7		FeII	177	2529.549	155
2532.0 2532.8		FeII		2533.627	110
2535.1		FeII	159	2536.803	140
2536.1					
2537.2		FeII	158	2538.799	100
2538.1				2538.909	100
				2538.993	125
2544.4 2545.0		NiII	18	2545.903	140
2548.0		FeII	145	2548.74	100
2554.0		NiII	62	2554.988	140
2556.25		ZnII:	3	2557.947	1000
2558.9		NiII	62	2560.156	120
2561.0 2561.7		FeII	64	2562.54	200
2562.6		FeII	2563.47		140
2565.4 2566.1		FeII	64	2566.91	60
2567.8		?			
2569.3		?			
2570.0		?			
2572.8 2573.55		FeII	144	2574.362	125
2575.25		MnII:	1	2576.105	1000
2577.1		FeII	64	2477.92	60
2580.95 2581.8		FeII	64	2582.580	100
2584.2 2585.0	1.7	FeII	1	2585.876	750
2586.2	0.5	FeII	1	2585.876	750

TABLE 2 (continued)

λ obs. (A)	FWHM (A)	ELEMENT	MULT.	λ lab. (A)	INT.
		IDENTIFICATIONS			
2590.0		FeII	64	2591.54	450
2590.8					
2592.3		FeII	64	2593.722	220
2592.9					
2594.15		?			
2597.5	2.7	FeII	1	2599.395	870
				2598.37	870
2599.75	0.5	FeII	1	2599.395	870
2605.2		FeII	1	2607.09	750
2606.0					
2610.1		FeII	1	2611.87	240
2611.0					
2612.5		FeII	1	2613.82	750
2613.05					
2616.0		FeII	2617.62		650
2616.85					
2619.85		FeII	1	2620.41	12
2620.9				2621.669	40
2620.85		FeII	1	2621.67	40
2623.9		FeII	1	2625.667	140
2624.75					
2626.6		FeII	1	2628.293	125
2627.45					
2629.5		FeII	1	2631.322	155
2630.4				2631.047	155
2663.0		CrII	8	2663.42	75
2663.9					
2665.0		CrII	8	2666.02	80
2665.8					
2683.15		FeII	283	2684.754	220
2683.9					
2691.0		CrII	84	2692.11	25
2691.85					
2700.8		FeIII	159	2701.13	220
2702.3		FeII	261	2703.988	60
2703.2					
2705.0		FeII	341	2706.566	220
2705.6					
2710.25		CrII	7	2712.30	80
2711.0					
2712.75		FeII	63	2714.41	80
2713.6					
2715.45		FeII	261	2716.217	50
			339	2716.429	40
2718.2		FeII	389	2719.301	12
2723.25		NiII		2724.725	50
2724.0					
2725.85		FeII	63	2727.54	80
2726.7					
2729.2		FeII	62	2730.734	40
2729.9					
2735.25		FeII	63	2736.98	650
2736.15					
2737.9	1.8	FeII	63	2739.54	200
2738.2					
2741.45	1.8	FeII	62	2743.20	140
2742.35					
2744.9		FeII	63	2746.98	870
2745.6		FeII	62	2746.483	170
2746.1					
2747.3		FeII	63	2749.18	750
2748.4				2749.48	220
2751.6		FeII	235	2753.287	80
2752.5					
2754.0		FeII	62	2755.73	280
2754.8					
2760.25		FeII	63	2761.812	125
2761.0					
2765.8		FeII	235	2767.50	750
2766.6			373	2767.500	750
2767.5		FeII	63	2768.934	12
2768.3					
2777.3		FeIII	2778.868		60
2777.75		FeII	234	2779.299	40
2778.4					
2782.0		FeII	234	2783.691	50
2782.7					
2789.4	1.3	MgII	3	2790.771	150
2793.3	3.0	MgII	1	2795.523	400
2795.9	0.6	MgII	1	2795.523	400
2800.5	3.0	MgII	1	2802.698	300
2803.1	0.5	MgII	1	2802.698	300
2830.0		FeII	217	2831.561	25
2830.8					
2834.4		CrII	5	2835.63	200
2839.0		CrII	82	2840.01	85
2839.7					
2841.9		FeII	294	2843.485	110
2842.4		CrII	5	2843.24	100
2842.7					
2847.15		FeII	317	2848.899	110
2847.7					
2848.2		CrII	5	2849.83	100
2849.0		FeIII	155	2850.288	120
2850.7		MgI	1	2852.127	1000
2852.5	0.3	MgI	1	2852.127	1000
2854.7		CrII	5	2855.67	100
2857.5		CrII	5	2858.91	75
				2858.655	30
2865.6		CrII	5	2866.72	100
2866.1					
2866.8		CrII	5	2867.65	100
2867.2					
2879.1		CrII	11	2880.86	75
2879.8					
2893.65		FeIII	125	2895.076	150
2924.8		FeII:	60	2926.586	10
2925.7					
2927.4		MgII	2	2928.635	80
2935.2	1.4	MgII	2	2936.501	100
2945.9		FeII	78	2847.66	750
2946.7					
2952.0		FeII	60	2953.774	550
2952.9					
2963.4		FeII	78	2964.629	360
			252	2964.131	220
2968.9		FeII	277	2969.934	285
2983.1	2.0	FeII	78	2985.545	750
2983.9					
3000.85		FeII	78	3002.650	750
3001.7					

The behaviour of the different elements and ions can be summarized as follows:

C I: The lines present are sharp, undisplaced, resonance lines (Fig. 1).

O I: This element is present in the resonance lines of multiplet 2 but they are blended with Si II; one can say for certain that O I displays relatively broad and also sharp components, and that its behaviour is definitely different than that of C I.

Mg II: The resonance lines (multiplet 1) display a P Cygni profile, the broad violet

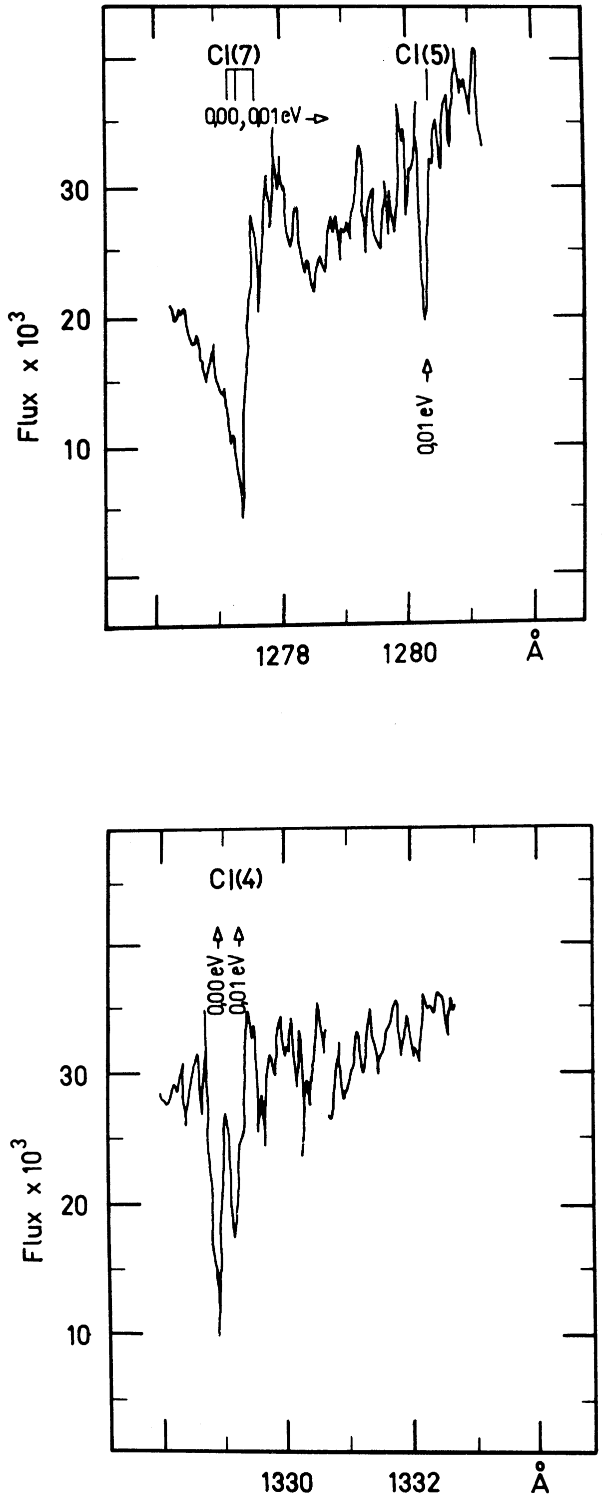

Fig. 1. The resonance lines of C I.

absorption (FWHM ∿3Å) being displaced by about -230 km/s. Actually, this absorption is very broad and we may be dealing with at least 2 components with velocities of approximately -300 and -175 km/s, respectively, values which in view of the uncertainties involved, could be considered similar to those from the absorption components in the photographic region. In addition, there is a sharp absorption at about +40 km/s. Subordinate lines of Mg II would seem to display two relatively broad absorption components. Figure 2 shows the resonance lines of Mg II.

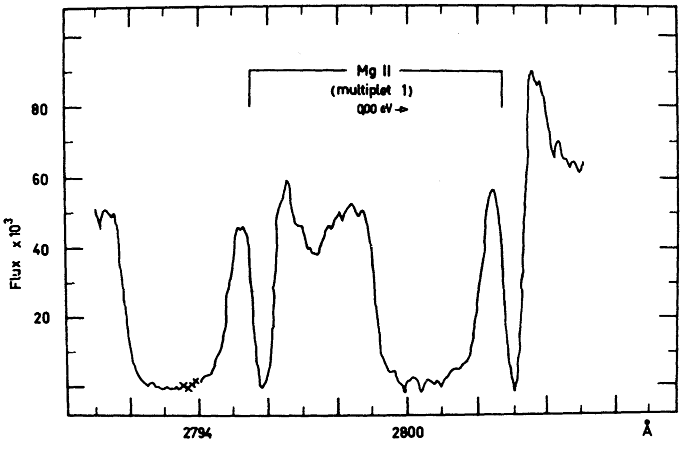

Fig. 2. The resonance lines of Mg II.

Al II: This ion displays a broad absorption feature (FWHM ∿ 1.2Å) at -120 km/s the lines arising from 0.00 eV level also display a sharp absorption at about +20 km/s.

Si II: Singly ionized silicon displays three components, a sharp one at about -300 km/s and two broad ones at -200 and at -120 km/s; the lines that arise from 0.00 eV level display, in addition, a sharp absorption at about +30 km/s (Fig. 3).

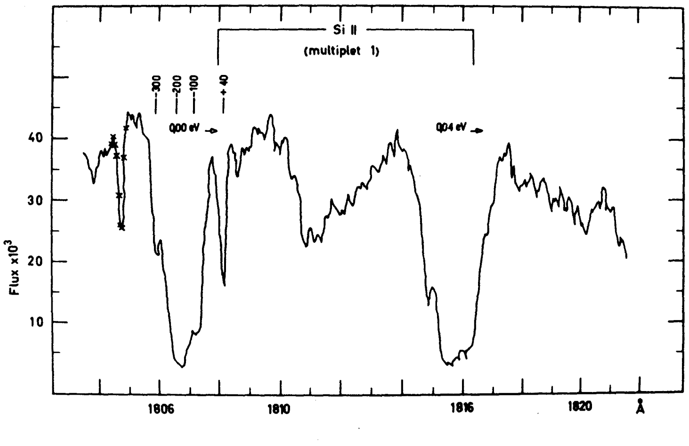

Fig. 3. The behaviour of Si II, multiplet 1.

S II: Singly ionized sulphur behaves like Si II.

Cr II: The lines of this ion are poorly defined; however, their behavior appears to be similar to that of Fe II.

Fe II: This ion displays two broad components at -200 and at -100 km/s; the lines arising from 0.00 eV level also display a sharp absorption at about +35 km/s (Fig. 4).

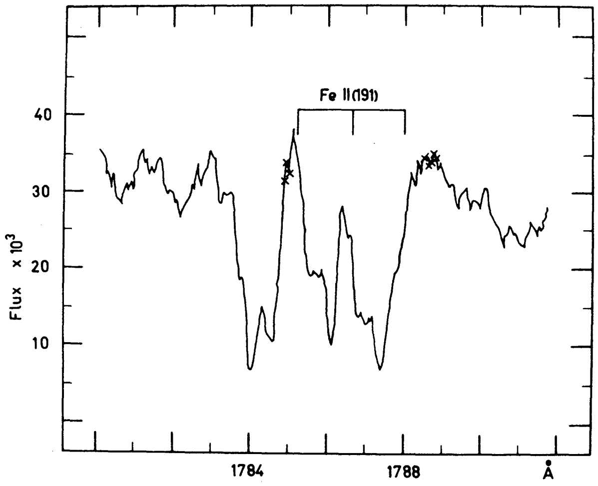

Fig. 4. Lines of Fe II.

Ni II: Singly ionized nickel displays three components, a sharp one at about -275 km/s and two broad ones at about -200 and -100 km/s, respectively; the resonance lines also display a sharp +25 km/s component (Fig. 5).

P III, Ti III, Fe III, Ni III: These ions display a single profile, with FWHM ∿ 1.4 Å, at about -200 km/s (Fig. 6). Ti III from 0.00 eV level displays also a sharp component at about +45 km/s; we cannot tell whether the same is true with the P III lines that arise from 0.00 eV level because they coincide with the resonance lines (multiplet 1) of C II. Fe III and Ni III have no resonance lines in the IUE wavelength range.

N V, C IV: These two ions display the two resonance components of multiplet 1, with apparently the same structure as the resonance lines of Si IV.

Si IV: Triply ionized silicon displays the two resonance lines of multiplet 1 and each one seems to show two relatively broad components at -200 and at +120 km/s. The latter measurement depends on the interpretation of the overall profile and, therefore, it is uncertain however, the actual value would seem to be, in any case, positive, and, as a consequence, in Table 3 we have entered the velocity value of +120: km/s for such a component, the profile of which may be asymmetric towards the longer wavelengths (Fig. 7).

Table 3 presents a summary of the behavior, velocity-wise, of the different elements and ions.

IV. DISCUSSION

Our study of the two IUE images of AX Mon shows conclusively that there is no contribution to the UV spectrum from the K component of the system and that no photospheric lines of the B companion appear to be present. Therefore, the UV line spectrum arises exclusively in the extended envelope in which the system is embedded.

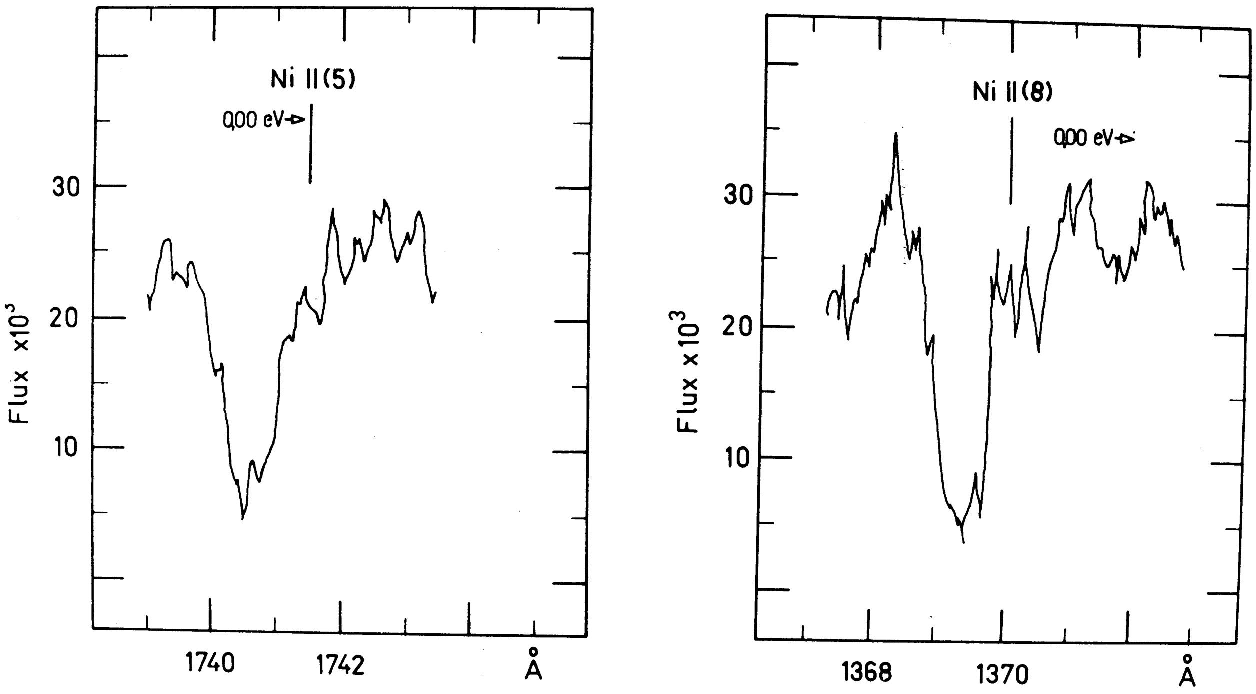

Fig. 5. The resonance lines of Ni II.

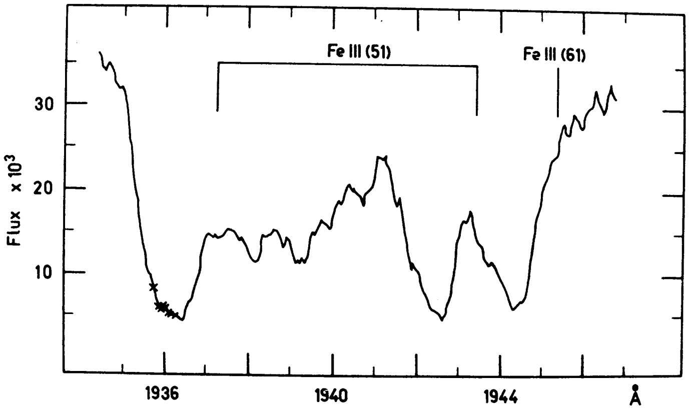

Fig. 6. Lines of Fe III.

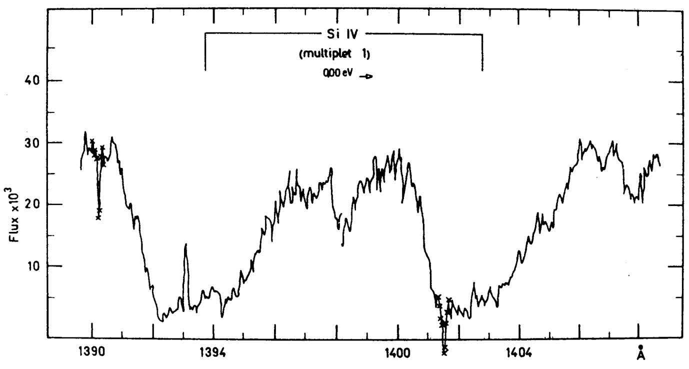

Fig. 7. The resonance lines of Si IV.

TABLE 3

VELOCITY BEHAVIOR OF SPECTRAL ABSORPTION LINES IN AX MONOCEROTIS

Element/Ion		Radial Velocity (in km/s)											
IUE	Photo-graphic	sharp comp.						Resonance Lines sharp components (0.00-0.01 eV)					
(H)	H*		-250		-150								
C I										0			
C IV								x					x
N V								x					x
O I								x:				x	
	Na I						x		x	+6?	+23		
Mg II*							-250:		-150:			+40	
Al II				x								+40	
Si II		-300		-200		-100	-300	-200	-100			+40	
Si IV								-200					+120
P III				-200									
S II		-300		-200		-100	-300	-200	-100			+40	
	Ca II						x		x	+6?	+24		
Ti III				-200									
Cr II				x		x						x	
Fe II				-200		-100		-200	-100			+40	
Fe III				-200									
Ni II			-250		-170	-100						+40	
Ni III				-200									

* P Cygni profiles. The velocities correspond to the violet absorptions.
x indicates probably present.
Figures derived from the photographic region were taken from Cowley (1964).

What can we conclude from observations that correspond to only one phase in the orbital cycle, namely, about 0.38P, counted from the conjunction at which the K star is in front?

1. Non-Thermal Sources

In the first place, we note that in AX Mon, as it has been true in other binary systems (Sahade and Ferrer 1982, Sahade and Hernández 1984a, b) and in symbiotic objects (Sahade, Brandi and Fontenla 1984), the line spectrum corresponds to a large range in electron temperature and some of these temperatures, like those that are required for the formation of the resonance lines of N V, C IV and Si IV, cannot be accounted for by the radiation field of either component of the system. This would suggest, here again, the existence of non-thermal sources of energy in the system.

2. High Electron Temperature Regions

In the second place, we have the fact that the resonance lines of Si IV display two broad components, one that yields a velocity of about -200 km/s and a second one that suggests a positive velocity. The existence of two components with very different velocities suggest, in turn, that there should be two regions of high electron temperature in the extended envelope of AX Mon. Because of the derived velocity values and because in other systems like β Lyrae (Hack *et al.* 1976) and AU Monocerotis (Sahade and Ferrer 1982) a similar conclusion has already been reached, we would be inclined to expect that the longward-displaced component of Si IV arises close to the stars, perhaps in the region where the gaseous stream from the K component interacts with the gaseous formation around the B-type companion (cf. Lubow and Shu 1975, Shu 1976). The asymmetry of this component towards long wavelengths, interpreted as indicating acceleration (Ringuelet 1983), would be an additional argument in support of our suggested location of the corresponding region of high electron temperature.

As far as the shortward-displaced component, we would like to suggest, also similarly as it was concluded in the cases of β Lyr (Hack *et al.* 1976), AU Mon (Sahade and Ferrer 1982) and γ_1 Velorum (Sahade and Hernández 1984a), that the corresponding high electron temperature region should be located at a certain distance from the stars and be perhaps related to the dissipation of shock waves produced in the area where gaseous matter is lost to the system through one of the external Lagrangian points (cf. Florkowski 1980). If we resort to the nomenclature used for the Sun, we can call *transition regions* the temperature-rise zones in the extended envelope of AX Mon where electron temperature increases at least up to the value required by the resonance lines of N V.

What about the rest of the lines?

3. The Interstellar Lines

The undisplaced resonance lines of C I must be of interstellar origin and, therefore, should be placed together with the interstellar lines of Ca II and Na I observed in the photographic region, outside the proper domain of the system.

4. The Outermost Layers of the Extended Envelope

The sharp component displayed by the resonance lines, arising in the 0.00 eV level, of O I, C II, Mg II, Al II, Si II, S II, Cr II?, Fe II, Ni II and Ti III, characterized by velocities in the range +20 to +40 km/s, should form in the outermost layers of the extended envelope. This is confirmed by the fact that H column density for Fe II comes out to be 6 x 10^{19} cm^{-2}. However, the possibility exists that some of the lines that yield velocities of the order of +20 km/s, may be of interstellar origin.

5. The Cool Shell

Although we have no way, so far, of establishing a distance scale in the extended envelope of AX Mon we can still try to place the positions of the regions where other ultraviolet lines originate, relative to those we have already discussed.

The P Cygni profiles of H in the photographic region, of Mg II (1) in the ultraviolet, and the non-interstellar, non-shell-like lines of Ca II in the photographic region are normally considered to originate in the so-called *cool shell* (Doazan and Thomas 1982) where the temperature should be of the order of 10^3 and the electron density perhaps 10^4 or 10^5 cm^{-3}. In AX Mon we observe two components of the violet absorptions and the question arises as to whether both components originate in the *post-transition region*. This would be the simplest assumption and would imply that the smaller velocity component would form further out than the larger velocity component, because the velocities at the *transition region* would be of the order of -200 km/s.

6. The |Fe II| Region

If we follow the presently accepted sequence of atmospheric regions in extended envelopes of a variety of stars (cf. Doazan and Thomas 1982, Kuhi 1983), we would further place the region where |Fe II| emission would originate, between the *cool shell* and the *outermost layers of the extended envelope*.

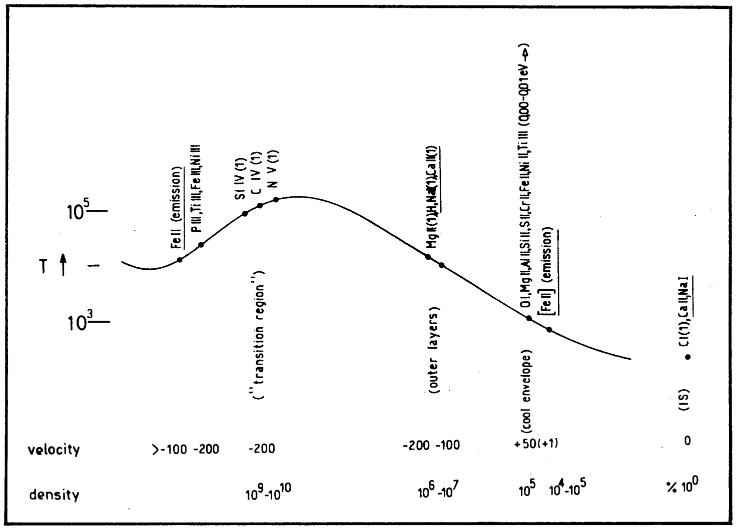

Fig. 8. Schematic model of the extended envelope of AX Monocerotis. The drawn temperature law curve and the distance scale are arbitrary. Information from the photographic region (Cowley 1964) is underlined.

Figure 8 depicts the location of the different regions we have mentioned, on an arbitrarily drawn temperature law curve, with an arbitrary distance scale. We still need to locate the region where the sharp component that is displayed by Si II, S II and Ni II at about -300 km/s originates from, the region of the subordinate lines of singly ionized elements, and also the region responsible for the lines of the doubly ionized elements. It is probable that the latter lines originate in the temperature-rise zone that precedes the *transition region*, and that the subordinate lines of singly ionized atoms form in a layer that is even closer in, but we need more information to ascertain whether all this is correct. Perhaps then we will be able to tell the relative location of the region where the photographic Fe II emission originates and whether such emission results from a geometrical or from a temperature effect (cf. Ringuelet *et al.* 1984).

We have at disposal only one IUE image of AX Mon and, then, it seems impossible to go any further in modelling the extended envelope around the system. It would certainly be necessary to have a good coverage of the orbital cycle if we wished to confirm and/or to improve upon our proposal, and perhaps even to understand the discrepancy between the luminosity class suggested for the early-type component by the photographic spectrum and the luminosity class suggested by the ultraviolet continuum. At any rate, we can at least say that the binary AX Mon, in spite of its complicated spectrum, seems to lead to a model for its extended envelope that is quite similar to those for other interacting binaries. It is interesting to point out, however, that, in our case, the observations suggest, in terms of the model, the existence in the extended envelope of a velocity plateau at -200 km/s, over quite a range in electron density.

We are indebted to Dr. Albert Boggess, then IUE Project Scientist, and to the IUE staff for their invaluable and most efficient help in acquiring and processing the images used in the present work. We are also very much indebted to Dr. George Wallerstein for useful comments.

REFERENCES

Batten, A.H., Fletcher, J.M. and Mann, P.J. 1978, *Pub. Dominion Astrophys. Obs.* 25, 121.
Burbidge, E.M. and Burbidge, G.R. 1954, *Ap. J.* 119, 501.
Cassatella, A., Ponz, D. and Selvelli, P.L. 1981, *IUE NASA Newsletter*, N°14, p. 170.
Cowley, A.P. 1964, *Ap. J.* 139, 817.
Doazan, V. and Thomas, R.N. 1982, in *B Stars with and without Emission Lines*, NASA SP-456,p.409.
Florkowski, D.R. 1980, in *Close Binary Stars: Observations and Interpretations, IAU Symposium № 88*, eds. M. Plavec, D.M. Popper and R.K. Ulrich (Dordrecht: Reidel), p. 229.
Hack, M., van den Heuvel, E.P.J., Hoekstra, R., de Jager, C. and Sahade, J. 1976, *Astr. Ap.* 50, 335.
Kuhi, L.V. 1983, in *Observational Basis for Velocity Fields in Stellar Atmospheres*, ed. R. Stalio (Trieste), p. 285.
Lubow, S.H. and Shu, F.H. 1975, *Ap. J.* 198, 383.
Pfeiffer, R. and Koch, R. 1977, *P.A.S.P.* 89, 147.
Ringuelet, A.E. 1983, private communication.
Ringuelet, A.E., Sahade, J., Rovira, M., Fontenla, J.M. and Kondo, Y. 1984, *Astr. Ap.* 131, 9.
Sahade, J., Brandi, E. and Fontenla, J.M. 1984, *Astr. Ap. Suppl. Series* 56, 17.
Sahade, J. and Ferrer, O.E. 1982, *P.A.S.P.* 94, 113.
Sahade, J. and Hernández, C.A. 1984a, *P.A.S.P.* 96, 88.
Sahade, J. and Hernández, C.A. 1984b, in preparation.
Serkowski, K. 1970, *Ap. J.* 160, 1083.
Shu, F.H. 1976, in *Structure and Evolution of Close Binary Systems, IAU Symposium № 73*, eds. P. Eggleton, S. Mitton and J. Whelan (Dordrecht: Reidel), p. 253.
Struve, O. 1943, *Ap. J.* 98, 212.
Swings, P. 1970, in *Spectroscopic Astrophysics*, ed. G.H. Herbig (U. of California Press), p.189.
Woodsworth, A. and Hughes, V.A. 1977, *Astr. Ap.* 58, 105.

Estela Brandi: Observatorio Astronómico de la Plata, Paseo del Bosque s/n., 1900 La Plata, Buenos Aires, Argentina.

Jorge Sahade: Instituto Argentino de Radioastronomía, C.C. 5, 1894 Villa Elisa, Buenos Aires, Argentina.